Alexandria Journal of Medicine

ISSN: 2090-5068 (Print) 2090-5076 (Online) Journal homepage: https://www.tandfonline.com/loi/tajm20

Role of proton magnetic resonance spectroscopy in diagnosis of pilocytic astrocytoma in children

Mohammed Mahmoud Donia, Ahmed Mohamed Abougabal, Yasser Mazloum Zakaria & Ahmed Hafez Farhoud

To cite this article: Mohammed Mahmoud Donia, Ahmed Mohamed Abougabal, Yasser Mazloum Zakaria & Ahmed Hafez Farhoud (2012) Role of proton magnetic resonance spectroscopy in diagnosis of pilocytic astrocytoma in children, Alexandria Journal of Medicine, 48:2, 131-137, DOI: 10.1016/j.ajme.2011.12.004

To link to this article: https://doi.org/10.1016/j.ajme.2011.12.004

Alexandria Journal of Medicine (2012) **48**, 131–137

Alexandria University Faculty of Medicine

Alexandria Journal of Medicine

www.sciencedirect.com

ORIGINAL ARTICLE

Role of proton magnetic resonance spectroscopy in diagnosis of pilocytic astrocytoma in children

Mohammed Mahmoud Donia [a,1], Ahmed Mohamed Abougabal [a,*], Yasser Mazloum Zakaria [a,2], Ahmed Hafez Farhoud [b,3]

[a] *Diagnostic Radiology Department, Faculty of Medicine, Alex University, Alex, Egypt*
[b] *Neurosurgery Department, Faculty of Medicine, Alex University, Alex, Egypt*

Received 4 December 2011; accepted 30 December 2011
Available online 23 January 2012

KEYWORDS

Pilocytic astrocytoma;
Magnetic resonance spectroscopy

Abstract *Background:* Pilocytic astrocytomas are the second overall most common pediatric brain tumor. Magnetic resonance (MR) imaging is widely used in the diagnosis and follow up of pediatric patients with pilocytic astrocytomas because of its ability to provide anatomical detail. However conventional MR imaging does not provide information about tissue biochemistry.
Aim of the work: To study the role of proton magnetic resonance spectroscopy in diagnosis of pilocytic astrocytoma in children.
Subjects and methods: This study included seven pediatric patients with histopathologically proven pilocytic astrocytoma. All patients were subjected to full history taking and thorough clinical examination. Magnetic resonance (MR) imaging was performed at 1.5 Tesla MR system using a standard head coil. Imaging included conventional MRI and proton magnetic resonance spectroscopy. Proton magnetic resonance spectroscopy was done using either single or multi-voxel technique. Surgical

Abbreviations: MRI, magnetic resonance imaging; MRS, magnetic resonance spectroscopy

* Corresponding author. Tel.: +20 01005048800.
E-mail addresses: donia1982@gmail.com (M.M. Donia), abougabal74@yahoo.com (A.M. Abougabal), yassermazloum@gmail.com (Y.M. Zakaria), a_farhoud@hotmail.com (A.H. Farhoud).
[1] Tel.: +20 01003989577.
[2] Tel.: +20 01222492447.
[3] Tel.: +20 01223130299.

Peer review under responsibility of Alexandria University Faculty of Medicine.
doi:10.1016/j.ajme.2011.12.004

Production and hosting by Elsevier

biopsy was then performed to all patients and correlation with histopathological data was done.
Results: Out of the seven patients included in this study, six were females and one was male with mean age of 9.5 years, the tumor was located in five of them in the posterior fossa, located in right thalamo-peduncular region in one patient and located in the hypothalamic–chiasmatic region in one patient.
MR spectroscopic study showed the same findings in all the lesions including high Cho/NAA and Cho/Cr ratios (3.53 ± 1.5) and (7.21 ± 4.2), respectively, relative low concentration of creatine with increased NAA/Cr ratio (2.32 ± 1.1). Lactate doublet was detected in all cases while no lipid peaks were detected.
Conclusion: Based on the findings in this study we suggest that pilocytic astrocytoma has a specific spectroscopic metabolic profile which could be diagnostic for this type of tumor.

1. Introduction

Pilocytic astrocytomas represent only 5–10% of all cerebral gliomas, but account for nearly about one third of the pediatric glial neoplasms. They are the second overall most common pediatric brain tumor. Their main locations are around the third and fourth ventricles. Nearly half are found in the optic chiasm and hypothalamus and about one third are located in the cerebellar vermis and hemispheres. Brain stem and basal ganglia are less common locations. They are typically tumors of children and young adults. Cerebellar tumors usually have a peak incidence at age of 10. Cerebral hemispheric tumors usually occur a decade later with a peak age of 20. Three quarters of optic pathway lesions occur under 12 years of age.[1]

Pilocytic astroctomas are well circumscribed but unencapsulated masses which are classified as WHO grade I. Their gross and radiological appearances vary according to location. Those located in the cerebellum tend to be cystic with internal solid mural nodule. Those located in the optic-hypothalamic region tend to be solid and well circumscribed while those located in the brainstem are usually solid and infiltrating and some time tend to be cystic.[2]

Magnetic resonance (MR) imaging is widely used in the diagnosis and follow up of pediatric patients with pilocytic astrocytomas because of its ability to provide anatomical detail. However conventional MR imaging does not provide information about tissue biochemistry.[3]

Proton MR spectroscopy is a non invasive in vivo technique that provides additional metabolic diagnostic indices beyond anatomic information and has been used widely in the imaging of brain tumors and other CNS pathologies. Several studies have shown that MR spectroscopy can help differentiate common pediatric brain tumors.[4]

The purpose of this study is to demonstrate different MR spectroscopic findings of pilocytic astrocytoma in children and to assess if there are certain specific spectroscopic findings which could be considered as diagnostic for this type of tumor.

2. Methods

The present study included seven patients in pediatric age group admitted to Alexandria university hospitals presenting with brain tumors histopathologically diagnosed as pilocytic astrocytomas after surgical biopsy.

All the patients were subjected to thorough history taking and clinical examination, conventional magnetic resonance imaging and magnetic resonance spectroscopic study. Correlation with histopathological data was done in all patients after surgical biopsy.

Magnetic resonance imaging was performed at 1.5 Tesla MR system using a standard head coil on Siemens Magnetom Avanto (Siemens, Erlangen, Germany). Patients were subjected to the following MRI protocols: Axial T2 weighted turbo spin echo (T2 TSE) (repetition time (TR) of 3000 ms, an echo time (TE) of 120 ms, a slice thickness of 4 mm, FOV = 230 × 230 mm), Axial T2 FLAIR (a repetition time (TR) of 8000 ms, an echo time (TE) of 100 ms, TI of 2200 ms, a slice thickness of 4 mm and FOV = 230 × 230 mm), pre-contrast axial T1 weighted spin echo (T1 SE) (a repetition time (TR) of 650 ms, an echo time (TE) of 15 ms, a slice thickness of 4 mm, FOV = 230 × 230 mm), axial, sagittal and coronal T1 weighted spin echo (T1 SE) after intravenous administration of 0.1 mmol/kg of dimeglumine gadopentate (Magnevist, Schering, Berlin, Germany). Patients who needed sedation were given the sedative dose of thiopental sodium 3 mg/kg. Incremental doses were given when needed.

Table 1 Summary of the spectroscopic MRI findings in the seven patients included in the study.

Case no.	Cho/NAA	Cho/Cr	NAA/Cr	Cr/Cho	Lactate	Lipids
1	1.35	3.56	2.62	0.27	+	–
2	2.17	7.63	3.50	0.13	+	–
3	3.30	9.41	2.85	0.11	+	–
4	3.02	4.18	1.38	0.24	+	–
5	4.18	12.75	3.03	0.08	+	–
6	4.66	11.32	2.64	0.09	+	–
7	6.07	1.64	0.27	0.61	+	–

Magnetic resonance spectroscopy (MRS) single or multi-voxel (CSI) was done by using point resolved spectroscopy (PRESS) sequences. Multi-voxel spectroscopy was performed using intermediate echo time of 135 ms (TR 1500 ms, FOV 160 mm) or short echo time of 30 ms (TR 1500 ms, FOV 160 mm) When multi-voxel spectroscopy was not possible because of the small size of the lesion, we used singe voxel spectroscopy (cubic voxel of 2 cm side length) of intermediate TE 135 ms (TR 1500 ms) or short TE 30 ms (TR 1500 ms).

Spectra were generated by the standard Siemens scanner software. Peak assignment was as follows: *N*-acetyl aspartate (NAA) at 2.0 ppm shift; choline (Cho) at 3.2 ppm; creatine (Cr) at 3.02 ppm and myo-inositol (mIns) at 3.65 ppm. The software also determined the area under each of these peaks by fitting them to standard curves. The areas under the peaks are proportional to the metabolite concentrations. Metabolite ratios (i.e. Cho/Cr, Cho/NAA, NAA/Cho, etc.) were calculated automatically by the workstation software.

3. Results

This study included seven patients with histopathological diagnosis of pilocytic astrocytoma, six were females and one was male with mean age of 9.5 years, the tumor was located in five of them in the posterior fossa, located in right thalamo-peduncular region in one patient and located in the hypothalamic–chiasmatic region in one patient.

3.1. Conventional MRI study

All the lesions showed heterogeneous signal with mixed solid and cystic components notably exhibiting hypointense signal in T1WI and hyperintense signal in T2WI. All of the lesions showed heterogeneous enhancement after contrast administration.

3.2. MRS analysis

- Increased Cho/NAA ratio; ranging from 1.35 to 6.07 with mean ratio 3.53 ± 1.5.
- Increased Cho/Cr ratio; ranging from 1.64 to 12.75 with mean ratio 7.21 ± 4.2.
- Increased NAA/Cr ratio; ranging from 0.27 to 3.5 with mean ratio 2.32 ± 1.1.
- Decreased Cr/Cho ratio; ranging from 0.08 to 0.61 with mean ratio 0.21 ± 0.19.
- Lactate doublet was detected in all cases.
- No lipid peak was detected.

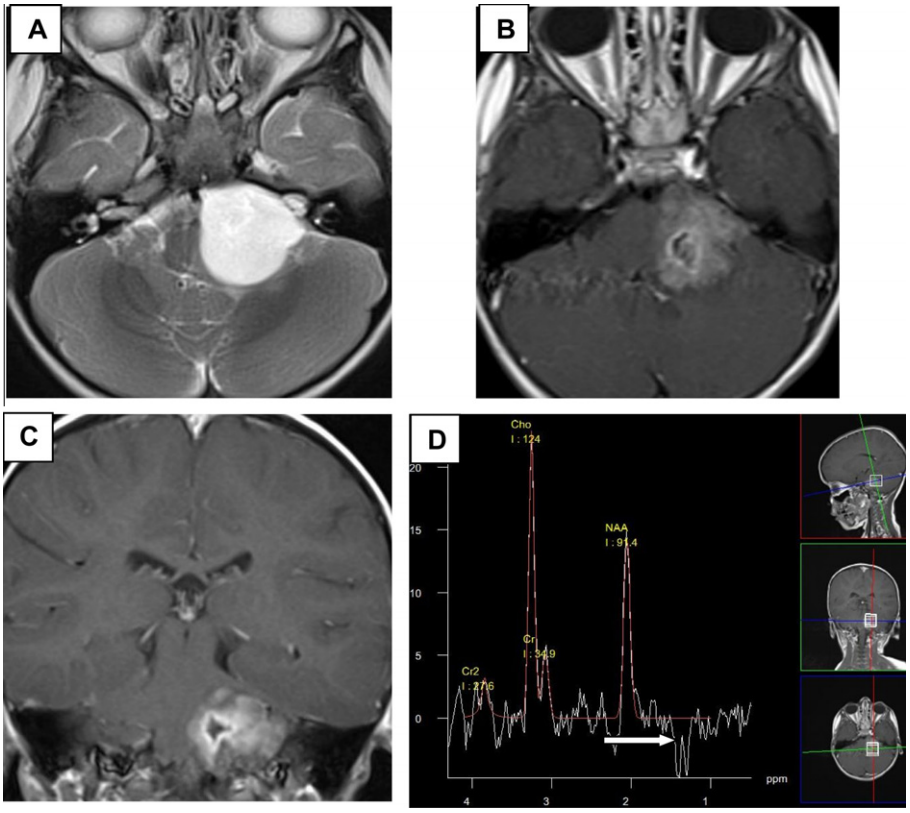

Figure 1 Case (1): A four-year-old female patient presented by gradual onset of disturbed consciousness, and left cranial nerve palsies. Axial T2WI (A), axial (B) and coronal (C) Gd-enhanced TIWI showed a well defined left sided CPA mass lesion with smooth outlines indenting and encroaching upon the brain stem and the left middle cerebellar peduncle. The lesion displayed T2 hyperintensity and heterogeneous enhancement after contrast administration with central non-enhancing component. Proton MRS (TE 144 ms) spectrum (d) revealed: high Cho/Cr ratio (3.56); high NAA/Cr ratio (2.62); lactate doublet at 1.3 ppm (arrow). Relatively low Cr concentration.

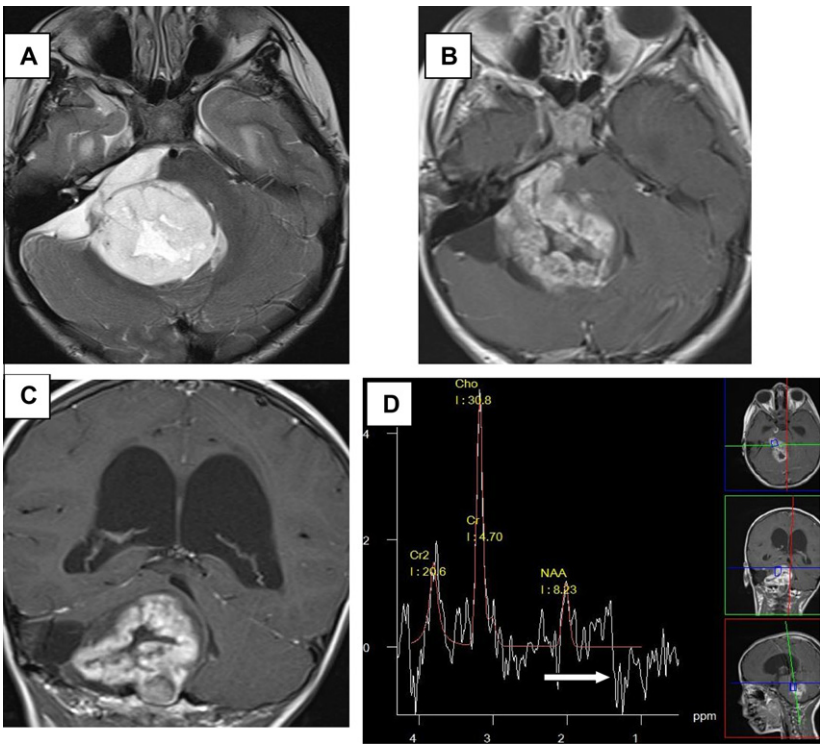

Figure 2 Case (2): A six-year-old female patient presented gradual onset of blurring of vision and disturbed gait. Axial T2WI (A), axial (B) and coronal (C) Gd-enhanced TIWI showed a well defined mass lesion involving in the right CPA and the right cerebellar hemisphere and indenting the brain stem. The mass displayed T2 hyperintensity and heterogeneous enhancement after contrast administration with central non-enhancing component. Proton MRS (TE 144 ms) spectrum (D) revealed: high Cho/Cr ratio (7.63); high NAA/Cr ratio (3.50); lactate doublet at 1.3 ppm (arrow). Relatively low Cr concentration.

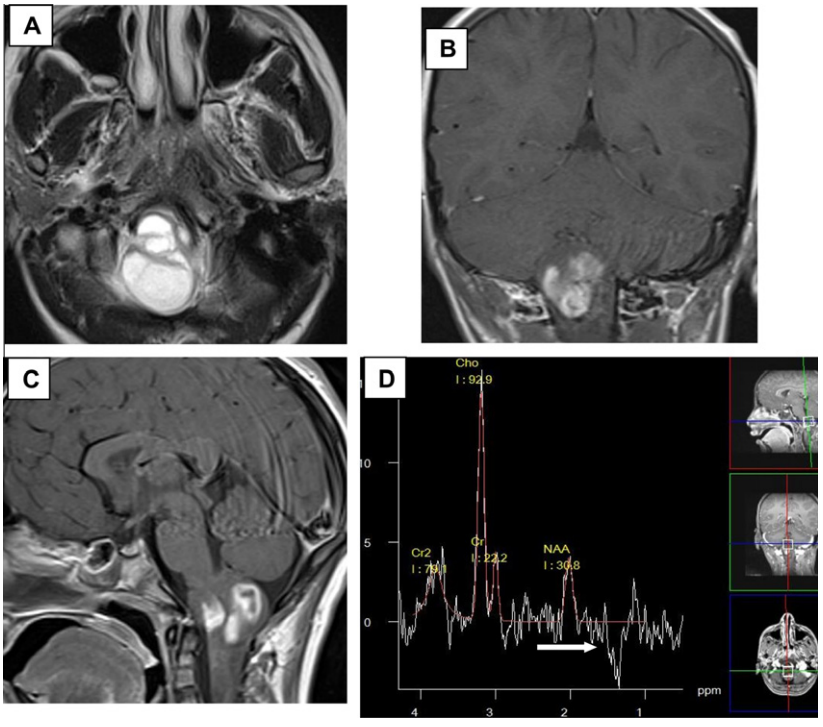

Figure 3 Case (3): A two-year-old female patient presented by disturbed level of consciousness. Axial T2WI (A), coronal (B) and sagittal (C) Gd-enhanced TIWI showed a sizable posteriorly exophytic mass lesion extending from the cervicomedullary region toward the cisterna magna. The lesion displayed T2 hyperintensity and heterogeneous enhancement after contrast administration. Proton MRS (TE 144 ms) spectrum (D) revealed: high Cho/Cr ratio (4.18); high NAA/Cr ratio (1.38); lactate doublet at 1.3 ppm (arrow). Relatively low Cr concentration.

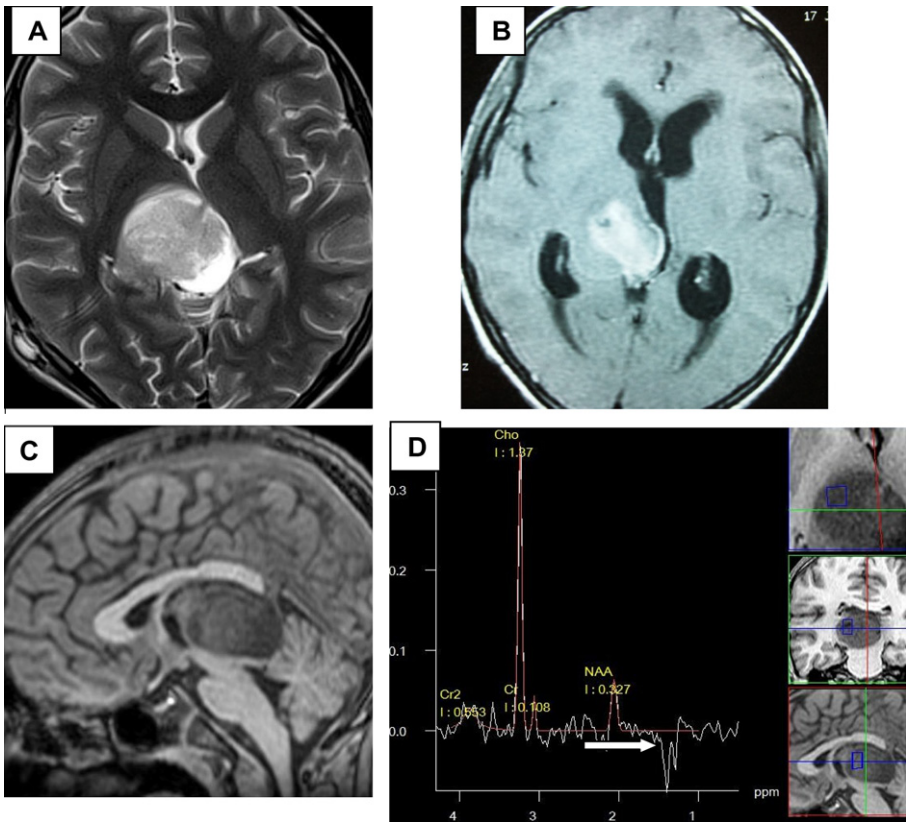

Figure 4 Case (4): A 15-year-old male patient presented by headache and disturbed level of consciousness. Axial T2WI (A), axial Gd-enhanced (B) and sagittal non-enhanced (C) TIWI showed right sided thalamo-peduncular mass lesion having a large solid and smaller cystic components, with mass effect upon the third ventricle with consequent mild hydrocephalic changes. The solid component displayed T2 hyperintensity, T1 hypointensity with homogenous intense enhancement after contrast administration. Proton MRS (TE 144 ms) spectrum (D) revealed: high Cho/Cr ratio (12.75); high NAA/Cr ratio (3.03); lactate doublet at 1.3 ppm (arrow). Relatively low Cr concentration.

Table 1 shows a summary of the spectroscopic MRI findings in the seven patients included in the study.

Figs. 1–5 show a demonstration for the MRI conventional and spectroscopic findings in five patients included in the study.

4. Discussion

In our study, we had seven patients with histopathologically proven pilocytic astrocytoma, five of them were in the posterior fossa and the remaining two were in supratentorial location and we found that pilocytic astrocytomas had specific metabolic profile that was demonstrated in all our cases, with no notable difference between supra- and infratentorial ones.

The spectra of pilocytic astrocytoma revealed high Cho/NAA and Cho/Cr ratios (3.53 ± 1.5) and (7.21 ± 4.2), respectively, relative low concentration of creatine with increased NAA/Cr ratio (2.32 ± 1.1). Lactate doublet was detected in all cases while no lipid peaks were detected.

Our results were in agreement with the previous studies which evaluated the role of MRS in the assessment of pilocytic astrocytoma.

Hwang et al.[5] found that pilocytic astrocytoma has relatively high Cho/NAA and Cho/Cr ratios (3.4 ± 2.14) and (3.46 ± 1.46) respectively with an elevated lactate doublet which was observed in all the studied cases. No dominant lipid peak was observed.

Cicel et al.[6] stated that pilocytic astrocytomas exhibit elevated lactate, and Cho and diminished levels of NAA, Cr, and mIns, and in contrast to Hwang et al.,[5] Cecil et al.[6] stated that elevated lipid was also found.

Our study was also in agreement with Panigrahy et al.[7] who found that the pilocytic astrocytoma had relatively low Cr and increased NAA/Cr ratio (1.8 ± 1.2) as compared to (2.32 ± 1.1) in our study.

Wang et al.[8] used long-echo-time MRS to classify pediatric cerebellar tumors with accuracy about 85% by using Cr/Cho and NAA/Cho ratios. They found low-grade astrocytomas and ependymomas had higher NAA/Cho ratio as compared to primitive neuroectodermal tumors.

An elevated lactate peak reflects anaerobic metabolism; surprisingly, this is not well correlated with tumor grade in the pediatric population.[6]

Kugel et al.[9] reported the lack of correlation between lactate signal and tumor grade. High lactate signal could be found in both benign and malignant tumors.[5]

Sutton et al.[10] found lactate peak in nearly all 25 pediatric gliomas studied, regardless of grade.

Multiple mechanisms were suggested by Hwang et al.[5] to explain the high lactate concentration in this benign tumor.

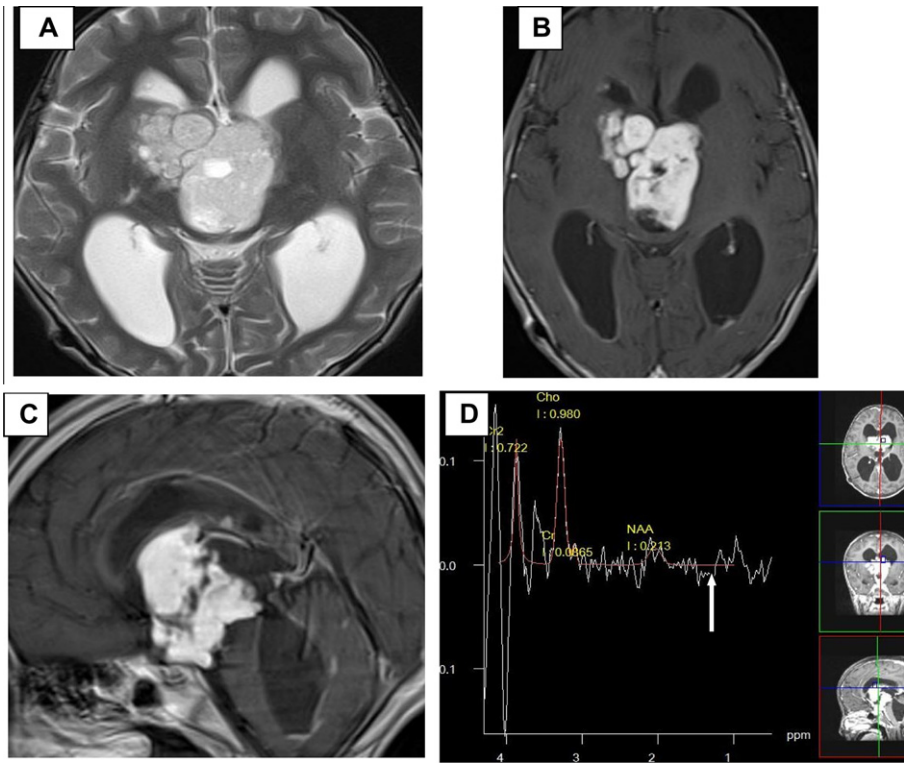

Figure 5 Case (5): A 13-year-old female patient presented by blurring of vision and vomiting. o Axial T2WI (A), axial (B) and sagittal (C) Gd-enhanced TIWI showed a sizable lobulated hypothalamic–chiasmatic mass lesion with intra-ventricular extension into the third and the lateral ventricle with consequent hydrocephalic changes. The lesion displayed T2 hyperintensity with intense enhancement after contrast administration. Proton MRS (TE 144 ms) spectrum (D) revealed: high Cho/Cr ratio (11.32); high NAA/Cr ratio(2.64); small lactate peak (arrow). Relatively low Cr concentration.

They suggested that high lactate concentration may be due to abnormal number or dysfunction of mitochondria, which would interfere with the process of oxidative phosphorylation and electron transport, alterations in proportional oxygen delivery, and oxygen extraction or usage by tumor or anaerobic glycolysis by tumor cells.

In three cases, and by using multi-voxel spectroscopy due to the large size of the lesions, we found no metabolic abnormalities outside the enhancing tumor bed reflecting its benign non aggressive behavior of this WHO grade I tumor. That was also demonstrated in a previous study by Morales et al.[11] who found an elevation in Cho/Cr ratios in the peritumoral regions of two cases of pilomyxoid astrocytoma in comparison with pilocytic astrocytoma, reflecting the more aggressive and infiltrative behavior of the former tumor.

Harris et al.[12] observed that the MRS spectra of pilocytic astrocytomas have low signal to noise ratio which may be due to their low cellularity compared with other tumors and this characteristic may be a useful discriminator for these tumors.

Finally based on the findings of our study in correlation with the findings of the previously mentioned studies we could suggest that pilocytic astrocytoma has a specific metabolic profile which is characterized by low creatine, elevated choline/creatine and *N*-acetyl aspartate/creatine ratios with the presence of lactate doublet at 1.3 p.p.m. So we recommend that MR spectroscopy should be a part of the routine MR examination for cases with suspected pilocytic astrocytoma as it could increase the imaging diagnostic efficiency of such tumors even before surgical removal and histopathological examination.

References

1. Tortori-Donati P, Rossi A, Biancheri R, Garrè ML, Cama A. *Brain Tumors. Pediatric Neuroradiology*. Berlin: Springer; 2005, p. 329–436.
2. Poussaint TY. *Diagnostic imaging of primary pediatric brain tumors. Diseases of the brain, head & neck, spine*. Berlin: Springer; 2008, p. 277–87.
3. Poussaint TY. Magnetic resonance imaging of pediatric brain tumors: state of the art. *Topics in Magnetic Resonance Imaging* 2001;**12**(6):411–33.
4. Soares DP, Law M. Magnetic resonance spectroscopy of the brain: review of metabolites and clinical applications. *Clin Radiol* 2009;**64**(1):12–21.
5. Hwang JH, Egnaczyk GF, Ballard E, Dunn RS, Holland SK, Ball Jr WS. Proton MR spectroscopic characteristics of pediatric pilocytic astrocytomas. *AJNR Am J Neuroradiol* 1998;**19**(3):535–40.
6. Cecil KM, Jones BV. Magnetic resonance spectroscopy of the pediatric brain. *Top Magn Reson Imaging* 2001;**12**(6):435–52.
7. Panigrahy A, Krieger MD, Gonzalez-Gomez I, Liu X, McComb JL, Finlay JL. Quantitative short echo time 1H-MR spectroscopy of untreated pediatric brain tumors: preoperative diagnosis and characterization. *AJNR Am J Neuroradiol* 2006;**27**(3):560–72.
8. Wang Z, Sutton LN, Cnaan A, Haselgrove JC, Rorke LB, Zhao H. Proton MR spectroscopy of pediatric cerebellar tumors. *AJNR Am J Neuroradiol* 1995;**16**(9):1821–33.

9. Kugel H, Heindel W, Ernestus RI, Bunke J, du Mesnil R, Friedmann G. Human brain tumors: spectral patterns detected with localized H-1 MR spectroscopy. *Radiology* 1992 Jun;**183**(3):701–9.
10. Sutton LN, Wang Z, Gusnard D, Lange B, Perilongo G, Bogdan AR. Proton magnetic resonance spectroscopy of pediatric brain tumors. *Neurosurgery* 1992;**31**(2):195–202.
11. Morales H, Kwock L, Castillo M. Magnetic resonance imaging and spectroscopy of pilomyxoid astrocytomas: case reports and comparison with pilocytic astrocytomas. *J Comput Assist Tomogr* 2007;**31**(5):682–7.
12. Harris LM, Davies N, MacPherson L, Foster K, Lateef S, Natarajan K. The use of short-echo-time 1 H MRS for childhood cerebellar tumours prior to histopathological diagnosis. *Pediatric Radiology* 2007;**37**(11):1101–9.